



Optimization of surface roughness in CO₂ laser ablation of aluminium-coated polymethyl methacrylate (PMMA) using response surface methodology

Job Lazarus Okello¹ · Ahmed M. R. Fath El-Bab² · Masahiko Yoshino³ · Hassan A. El-Hofy^{1,4}

Received: 30 November 2022 / Accepted: 28 April 2023 / Published online: 15 May 2023
© The Author(s), under exclusive licence to Springer Nature Switzerland AG 2023

Abstract

The growth of microfluidics has significantly increased the demand for microfluidic products. CO₂ lasers are employed to manufacture microfluidic devices using polymethyl methacrylate (PMMA) because of flexibility, time- and cost-effectiveness. However, optimization and defining the relationships among the parameters are challenging. High surface roughness negatively affects the quality of microfluidic devices. This work employed response surface methodology to investigate the effects of power (1.5, 3.0, and 4.5 W), speed (10, 15, and 20 mm/s), and pulse rate (800, 900, and 1000 pulses per inch) on surface roughness in CO₂ laser fabrication of microchannels on PMMA coated with a 500 nm layer of 99.95% pure aluminium. A full quadratic model was developed. Analysis of variance (ANOVA) and optimization were done. Power is the most significant factor followed by speed and pulse rate. The optimization results were validated experimentally. The developed model is highly accurate with an absolute percentage error of 2.617%. Manufacturing engineers can use it to efficiently predict surface roughness values.

Keywords Aluminium coating · CO₂ laser ablation · Optimization · Polymethyl methacrylate (PMMA) · Response surface methodology · Surface roughness

1 Introduction

Microfluidics is an on-demand technology that uses microchannels for handling fluids in various microfluidic devices (Helmy et al. 2018; Aravind et al. 2021; Konari et al. 2021). Microchannels are being heavily employed in various applications like micro-total analysis systems, chromatography, implantable devices, inkjet printers, blood

analysis, environmental assessment, binary storage devices, and telecommunication (Prakash et al. 2013; Dudala et al. 2019). There has been significant growth in the use of microfluidic devices in several applications in life science, engineering, medical, biochemical analyses, and other areas (Aravind et al. 2021; Helmy et al. 2015; Prakash and Kumar 2015).

CO₂ lasers are being heavily used to fabricate many types of microchannels on various polymers for different kinds of microfluidic applications (Prakash and Kumar 2018). CO₂ laser fabrication is a flexible, efficient, versatile, fast, and cheap technique for creating microstructures in many materials. Also, no tool change is required. Hence, tool wear is not an issue (Dudala et al. 2019; Helmy et al. 2015). The availability and low cost of PMMA and CO₂ laser fabrication make single-use microfluidic devices fabricated using PMMA disposable as required in various applications (Nasser et al. 2018).

During direct CO₂ laser ablation, the PMMA material evaporates and melts due to the high temperature of the laser projected area. This leads to distortion and thermal

✉ Job Lazarus Okello
job.okello@ejust.edu.eg

¹ Industrial and Manufacturing Engineering Department, Egypt-Japan University of Science and Technology, New Borg El-Arab City, Egypt

² Mechatronics and Robotics Engineering Department, Egypt-Japan University of Science and Technology, New Borg El-Arab City, Egypt

³ Department of Mechanical Engineering, Tokyo Institute of Technology, Tokyo, Japan

⁴ On leave from Department of Production Engineering, Faculty of Engineering, Alexandria University, Alexandria, Egypt

defects in the form of bulges, heat-affected zone (HAZ), clogging, and high surface roughness (Helmy et al. 2015, 2018). Also, when heated, PMMA changes its phase after which it melts and consequently vaporizes at different temperatures (Khamar and Prakash 2020). It is also very hard to achieve accurate dimensional control because of the variations in the values of the thermal and physical properties of PMMA during CO₂ laser micromachining (Ali et al. 2015). The defects must be overcome to get high-quality microchannels and improve the bonding capacity and the fluid-mixing efficiency of the microfluidic devices fabricated using PMMA substrates (Helmy et al. 2018; Prakash and Kumar 2017). The defects can be overcome by controlling the inputs and coating the PMMA substrates before fabricating the microchannels (Helmy et al. 2015, 2018; Okello et al. 2022).

In a multivariate scheme such as laser micromachining, defining the relationships among the various parameters is often tedious. Accordingly, controlling the inputs is a serious hurdle (Helmy et al. 2018). Conducting experiments using trial-and-error is time-consuming and does not take care of the interactions among the parameters leading to many errors (Moradi et al. 2017). Techniques of design of experiments (DoE) like the Taguchi method, response surface methodology (RSM), and full factorial design are used to design and conduct experiments. With the techniques, many parameters can be varied simultaneously, modelled, and optimized. Consequently, the inputs can be controlled to get the desired values of the outputs (Hao et al. 2013; Benton et al. 2019).

Several studies have been conducted on CO₂ laser micromachining of PMMA using DoE techniques to examine how the inputs affect the responses and develop relationships between the inputs and outputs to get the optimum results (Moradi et al. 2017; Oladoye et al. 2016; Eltawahni et al. 2010). Helmy et al. (2018) carried out the fabrication and characterization of PMMA microchannel using CO₂ laser in both air and underwater. They carried out multi-objective optimization of surface roughness, microchannel width, depth, aspect ratio, and heat-affected zone using Taguchi's experimental design with grey relational analysis. They conducted 9 experiments in air and 9 underwater by leaving a 300 μm water layer on the top surface of the PMMA substrate. They studied the effect of scanning speed and laser power on surface roughness, HAZ, and aspect ratio. They found that the cooling effect of ablation underwater significantly decreases the extent of thermal damage but increases the aspect ratio. Using ANOVA, they found laser power to be the most significant factor followed by the scanning speed and pulse rate. For both the fabrication in air and underwater, they found that the scanning speed of 20 mm/s, laser power of 3 W, and 900 PPI is the optimum combination of the process parameters. They confirmed the optimization results by conducting a validation experiment at the optimum condition.

Using response surface methodology (RSM), Umbrecht et al. (2009) fabricated and characterized microchannels of 130 μm width and 4 μm depth on PMMA by applying a novel solvent-assisted bonding. They examined the bonding pressure, bonding temperature, the time for which the solvent was applied to the PMMA substrates, and the time for the application of the pressure and temperature. They reported high strengths of bonds (3.5 ± 0.8 MPa) at low deformations ($1.6 \pm 0.3\%$) at the center point of the DoE. They integrated the bonding process in the fabrication of a wireless implantable strain sensor and reported that the bonding was validated by ultrasound measurements. They found the predicted values of the bond deformation and strength to agree with the experimental values.

Choudhury and Shirley (2010) used RSM and studied CO₂ laser micromachining of PMMA, polycarbonate (PC), and polypropylene (PP). The inputs were the air pressure, cutting speed, and laser power while the responses were surface roughness, dimensional accuracy, and heat-affected zone (HAZ). Using the central composite design, they carried out 12 tests for individual polymers and developed first-order linear models for surface roughness and HAZ. They tested the adequacy of the models using analysis of variance (ANOVA). The models were found to adequately predict the values of surface roughness and HAZ. They found less HAZ in PMMA proceeded by PC and PP. PMMA also had better surface quality than both PC and PP. Dimensional accuracy was determined by the deviation of the real value from the supposed value. The dimensional deviation was maximum in PMMA followed by PP and least in PC. HAZ was found to be inversely proportional to both compressed air pressure and speed but directly proportional to power. Compressed air and speed were found to be more significant than power.

Prakash and Kumar (2015) investigated the effects of laser power, number of pulses, and scanning speed on the softened zone, microchannel width, and microchannel depth in CO₂ laser ablation of PMMA. They performed 27 experiments using a 3-level full factorial experimental design and carried out mathematical modelling of each parameter using nonlinear regression analysis. They also performed multi-objective optimization and conducted a confirmation experiment to verify the optimization results. They found that the presence of a softened zone plays a significant role in fabricating microfluidic devices on PMMA because it leads to bulges. They further found that even a slight change in laser power predominantly affects all three microchannel characteristics. The predicted models can readily be used to predict the microchannel dimensions for the inputs.

In this work, RSM was used to study surface roughness in CO₂ laser ablation of microchannels on PMMA coated with a 500 nm layer of 99.95% pure aluminium. The inputs were pulse rate, power, and speed. The experiments were designed using Minitab® 19.1 software and the results were

also analyzed using the software. A mathematical model was developed and tested. ANOVA was performed to determine the significance of the inputs. Optimization of surface roughness was done, and the results were validated.

2 Materials and methods

2.1 Materials

A 6-mm thick transparent PMMA sheet was used in this work. A 1-mm diameter aluminium wire of purity 99.95% was used for coating the PMMA samples. After the fabrication of the microchannels, the aluminium coating was etched using an aluminium etchant and the samples were cleaned using Acetone and then washed using ethanol.

2.2 Methods

Fabrication of the microchannels was done using the 30-W Universal CO₂ Laser machine, VLS 3.5, USA. The maximum resolution of the machine is 1000 pulses per inch (PPI) while the maximum speed is 250 mm/s. A total of 18, 30 mm × 25 mm × 6 mm PMMA work samples were cut from a PMMA sheet using the laser machine. The samples were then cleaned using water to remove the impurities and dirt that could negatively affect the results of the fabrication (Konari et al. 2021). Through sputtering, the samples were coated with a 500 nm layer of 99.95% pure aluminium using NANOVAK® Thermal and Sputtering Combined Systems, (NVTS-400-2TH2SP). The deposition was done in a cleanroom of class 10,000. The desired microchannels were first drawn using CorelDRAW® Graphics Suite X5 and then fabricated in a single laser pass following the deposition of aluminium on the work samples.

The room's temperature was set to and maintained at 25 °C using an air conditioning system. The laser power was kept low since previous studies have proved that for the fabrication of microchannels on PMMA using CO₂ laser, low power gives the best microchannel quality (Helmy et al. 2015, 2018). After the fabrication, the samples were immersed in Ethanol and washed for 20 min in an ultrasonic cleaner to get rid of the particles that were stuck on the samples during the fabrication (Helmy et al. 2015, 2018). The aluminium coating was then etched using an aluminium etchant.

Before analyzing the microchannels, the samples were properly washed using deionized water and then left to dry. The microchannels were carefully measured with the 3D laser microscope, KEYENCE VK- × 100. With the microscope, measurements are conducted without contact with the sample. The resolution of the microscope is at the nanometer level. The microscope takes measurements by scanning the surfaces of materials. It then produces optical and 3D

Table 1 The inputs and their levels

Variable	Coded			Actual		
	Low	Mid	High	Low	Mid	High
Speed (mm/s)	− 1	0	1	10	15	20
Power (W)	− 1	0	1	1.5	3.0	4.5
Pulse Rate (PPI)	− 1	0	1	800	900	1000

images with high resolutions. To determine the nanometer level heights, the intensity of the laser light is examined with the datum being the laser's z-position. The sample to be measured is carefully put on the stage of the microscope and properly altered together with the microscope until a sharp focus is obtained. Measurements are then done. The software of the microscope then produces measurement data that can be evaluated as necessary (Okello et al. 2022).

Surface roughness (Ra) was measured using the microscope at the base of each microchannel. For precise results, measurements were conducted thrice at different points and the mean values were used (Helmy et al. 2015, 2018). Response surface methodology was used to design the experiments in Minitab® 19.1. The high, middle, and low levels were selected for speed (mm/s), power (W), and pulse rate (PPI). Table 1 shows the inputs and their coded and actual design levels.

Central composite design (CCD) with $\alpha = 1.682$ was used with three parameters: power, speed and pulse rate. The design includes 18 experiments with 8 experiments as factorial points in the cubic vertex, 6 experiments as axial points, and 4 experiments as the center point experiments. The 18 experiments were replicated thrice hence a total of 54 experiments were conducted. The 54 experiments allowed the estimation of the quadratic, linear as well as interactive effects of the inputs on the responses. The variables were coded using Minitab® 19.1 software. The software was also used to analyse the results and produce the response surface graphs and then optimize the parameters. Using the full quadratic polynomial function, analysis of variance (ANOVA) was utilized to assess the adequacy of the developed models and get the significant parameters, and further interpret the results (Moradi et al. 2017; Oladoye et al. 2016).

3 Results and discussion

3.1 Effects of the inputs on surface roughness

Figures 1 and 2 respectively show the profile and the optical image of the microchannel obtained at 3.0 W, 15 mm/s, and 900 PPI. Values of surface roughness (Ra) ranged from 7.134 μm, got at 1.5 W, 20 mm/s, and 1000 PPI, to

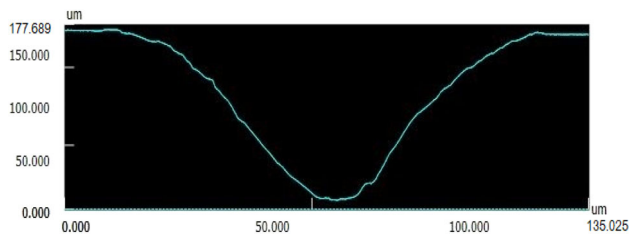


Fig. 1 Profile of the microchannel obtained at 3.0 W, 15 mm/s, and 900 PPI

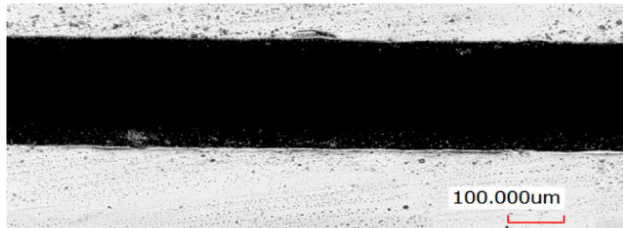


Fig. 2 Optical image of the microchannel obtained at 3.0 W, 15 mm/s, and 900 PPI

44.267 μm , obtained at 4.5 W, 10 mm/s, and 800 PPI. The experimental results are shown in Table 2.

As shown in the main effects plot (Fig. 3), interaction plots (Fig. 4), and surface plots (Fig. 5), both the individual inputs and their interactions affect surface roughness. Figures 3, 4, and 5 all indicate that when power increases and both speed and pulse rate decrease, surface roughness increases. However, when power decreases and both speed and pulse rate increase, surface roughness decreases. Thus, low values of surface roughness are attained at low power and high speed, and pulse rate. Figure 4 shows that the interaction between power and speed produces the strongest effects on surface roughness in comparison with the interaction between pulse rate and speed, and pulse rate and power.

When power is high and both speed and pulse rate are low, the amount of heat input is high. Thus, the PMMA substrates absorb a large amount of heat. Due to the low values of speed, the laser beam interacts with the PMMA substrates for a long time. The substrates get heated up, melt, decompose, cool, and then resolidify at high rates. High surface roughness results. The resulting surface finish is poor and the microchannels have poor quality (Helmy et al. 2018; Okello et al. 2022; Imran et al. 2021).

Conversely, when power is low and both speed and pulse rate are high, the amount of heat input is low. Therefore, the PMMA substrates absorb a small amount of heat. Owing to the high values of speed, the laser beam interacts with the substrates for a short time. The substrates get heated up, melt, decompose, cool, and resolidify at low rates. Low surface roughness results. Also, the surface finish is good and the

Table 2 Experimental results

Run order	Power (W)	Speed (mm/s)	Pulse rate (PPI)	Ra (μm)
1	3.0	15	900	10.101
2	1.5	10	800	8.642
3	3.0	15	800	12.607
4	3.0	15	900	11.051
5	3.0	15	900	10.905
6	4.5	20	1000	23.549
7	4.5	10	800	44.267
8	1.5	15	900	7.614
9	4.5	20	1000	24.957
10	1.5	10	1000	7.942
11	1.5	20	800	7.302
12	1.5	10	1000	7.933
13	1.5	10	1000	7.951
14	3.0	15	900	10.668
15	4.5	20	800	26.009
16	3.0	15	900	11.114
17	4.5	20	800	27.014
18	3.0	20	900	8.919
19	3.0	15	900	10.851
20	3.0	10	900	17.513
21	3.0	15	900	11.009
22	4.5	10	1000	38.201
23	1.5	15	900	7.598
24	3.0	15	1000	9.136
25	4.5	10	1000	40.628
26	1.5	20	800	7.245
27	4.5	15	900	33.282
28	3.0	15	900	11.117
29	3.0	15	900	10.975
30	1.5	10	800	8.651
31	3.0	20	900	8.915
32	4.5	10	800	42.518
33	3.0	15	800	12.514
34	1.5	10	800	8.661
35	1.5	20	1000	7.138
36	3.0	20	900	8.921
37	4.5	20	800	26.125
38	4.5	15	900	33.436
39	3.0	15	1000	9.114
40	4.5	15	900	32.104
41	3.0	10	900	16.715
42	4.5	10	800	43.237
43	1.5	20	1000	7.134
44	3.0	15	800	12.418
45	3.0	15	900	11.157

Table 2 (continued)

Run order	Power (W)	Speed (mm/s)	Pulse rate (PPI)	Ra (μm)
46	1.5	20	1000	7.141
47	3.0	10	900	17.402
48	3.0	15	900	10.899
49	4.5	10	1000	39.753
50	1.5	15	900	7.528
51	1.5	20	800	7.321
52	4.5	20	1000	24.009
53	3.0	15	1000	9.124
54	3.0	15	900	11.113

therefore, restricted leading to poor results in analyses. Conversely, fluids flowing through microchannels that have low surface roughness experience little resistance. They are, therefore, less restricted leading to better results of analyses. The values of power should be low, and the values of both pulse rate and speed should be high to have low heat input and, therefore, attain microchannels with low surface roughness and, therefore, good quality (Helmy et al. 2015, 2018; Madić et al. 2020). In microfluidics, surface roughness should be low for highly efficient results of analyses (Helmy et al. 2018; Okello et al. 2022).

microchannels have good quality (Helmy et al. 2015, 2018; Okello et al. 2022).

Fluids flowing through microchannels that have high surface roughness experience a lot of resistance. They are,

3.2 Modelling of surface roughness

Four models were obtained using Minitab® 19.1: linear, linear + squares, linear + interactions, and full quadratic. The highest value of the predicted determination coefficient R^2 was used to select the most accurate model because the higher

Fig. 3 Main effects plot for surface roughness

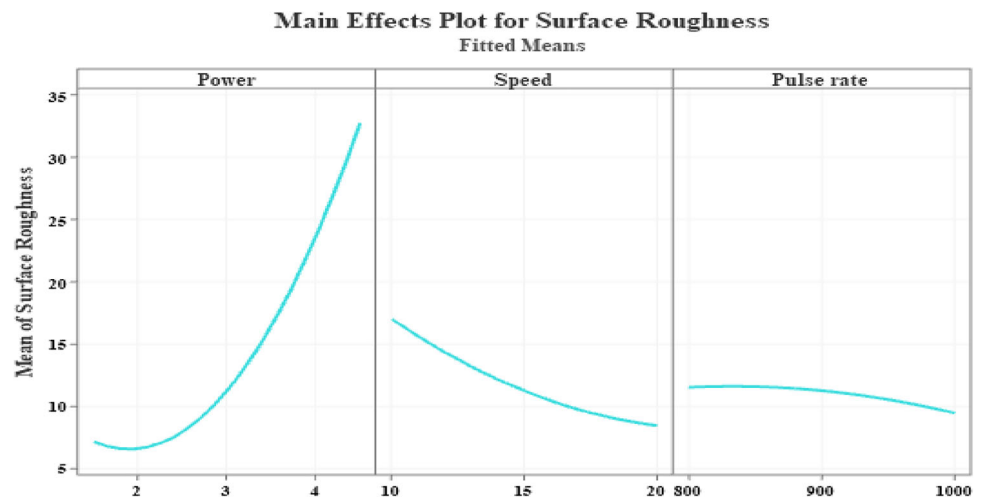
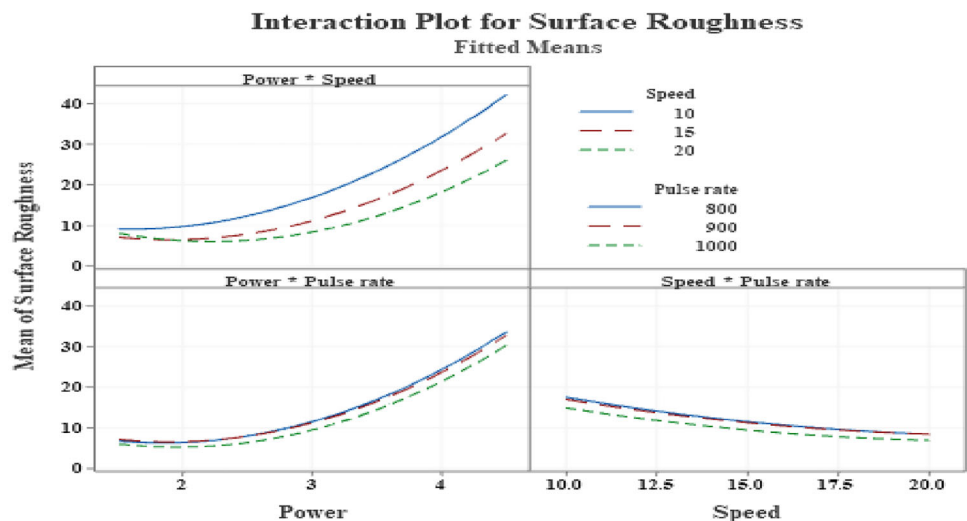


Fig. 4 Interaction plot for surface roughness



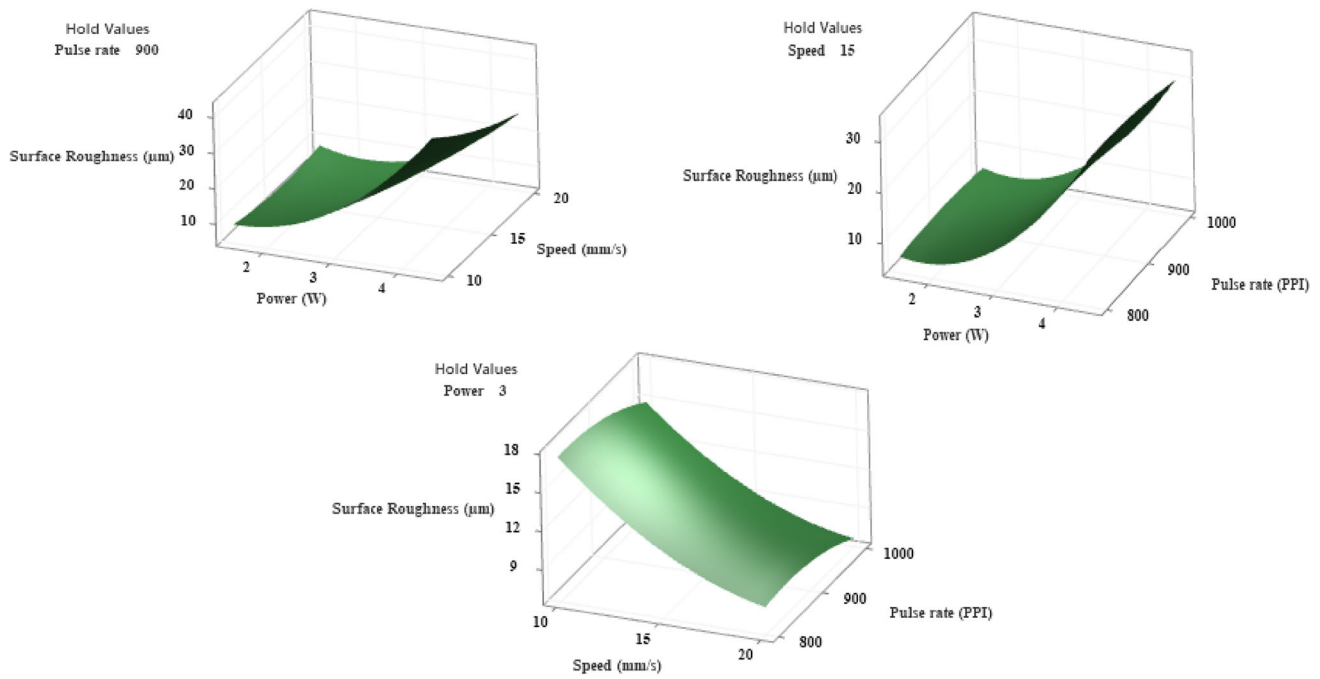


Fig. 5 Surface plots for surface roughness

Table 3 Model summary statistics

Model	s	R-sq	R-sq(adj)	R-sq(pred)
Linear	5.447210	78.69%	77.41%	74.78%
Linear + interactions	4.905560	83.75%	81.68%	78.59%
Linear + squares	2.800680	94.70%	94.03%	92.84%
Full quadratic	0.604697	99.77%	99.72%	99.63% Selected

the value of the predicted R^2 of a model, the higher the accuracy of the model to predict the value of a response. The quadratic model best predicts the values of surface roughness because it has the highest values of R^2 , adjusted R^2 , and predicted R^2 compared to all the other models as shown in Table 3.

The values of R^2 , adjusted R^2 , and predicted R^2 are all close to 1 indicating that the model is highly adequate for predicting the values of surface roughness. The regression model (Eq. 1) was generated in Minitab® 19.1 using the selected full quadratic model. The insignificant terms were excluded to improve the accuracy of the model (Acherjee et al. 2012). In the regression model, Ra represents average surface roughness while X_1 , X_2 , and X_3 denote power, speed, and pulse rate respectively.

$$Ra = -33.1 - 3.209X_1 - 1.610X_2 + 0.1323X_3 + 3.856X_1^2 + 0.05919X_2^2 - 0.000077X_3^2 - 0.5025X_1X_2 - 0.004303X_1X_3 + 0.00054X_2X_3 \quad (1)$$

3.3 Analysis of variance (ANOVA) of surface roughness

ANOVA was performed to find out the significance of the inputs and determine their influence on surface roughness. To determine the significance of the inputs, the p-value statistical factor is used. A factor is significant if its p-value is less than or equal to 0.05 otherwise, it is not significant (Abidi et al. 2021). ANOVA alongside the lack-of-fit and F-tests help to determine the accuracy of the models for predicting the values of the given output responses (Okello et al. 2022). According to the ANOVA results, the quadratic model best predicts the values of surface roughness for any set of values of the inputs. As shown in Table 4, all the factors are significant. The most significant one is the laser power with a 70.35% contribution followed by speed (7.88%), the square of power (8.79%), the interaction between power and speed (4.90%), pulse rate (0.45%), the square of speed (0.26%), the interaction between power and pulse rate (0.14%), the square of pulse rate (0.07%) and interaction between speed and pulse rate (0.03%).

Table 4 ANOVA of surface roughness

Source	DF	Adj SS	Adj MS	F-Value	P-Value	Percentage contribution
Model	9	6944.99	771.67	2110.34	0.000	99.76885771
Linear	3	5477.48	1825.83	4993.25	0.000	78.6872152
Power	1	4896.99	4896.99	13,392.2	0.000	70.34813563
Speed	1	548.82	548.82	1500.92	0.000	7.884121429
Pulse rate	1	31.66	31.66	86.6	0.000	0.454814483
Square	3	1114.94	371.65	1016.38	0.000	16.01676751
Power*Power	1	611.9	611.9	1673.41	0.000	8.790302654
Speed*Speed	1	17.8	17.8	48.69	0.000	0.255707448
Pulse rate*Pulse rate	1	4.76	4.76	13.03	0.001	0.068380194
2-Way Interaction	3	352.57	117.52	321.4	0.000	5.064874991
Power*Speed	1	340.82	340.82	932.08	0.000	4.896079344
Power*Pulse rate	1	10	10	27.34	0.000	0.143655869
Speed*Pulse rate	1	1.75	1.75	4.78	0.034	0.025139777
Error	44	16.09	0.37			0.231142294
Lack-of-Fit	5	7.49	1.5	6.79	0.000	0.107598246
Pure Error	39	8.6	0.22			0.123544048
Total	53	6961.08				

3.4 Optimization of surface roughness

Optimization was done to find out the optimum value of the inputs and surface roughness. Three possible solutions were generated in Minitab® 19.1 and the solution with the highest value of composite desirability was selected as the best. The higher the value of the desirability, the better the solution (Abidi et al. 2021). Good microchannels require good surface integrity and, hence, low surface roughness (Helmy et al. 2018). Therefore, surface roughness was minimized. Figure 6 shows that the minimum value of surface roughness (4.7759 μm) can be got at the optimum conditions: 2.1667 W, 18.2828 mm/s, and 1000 PPI.

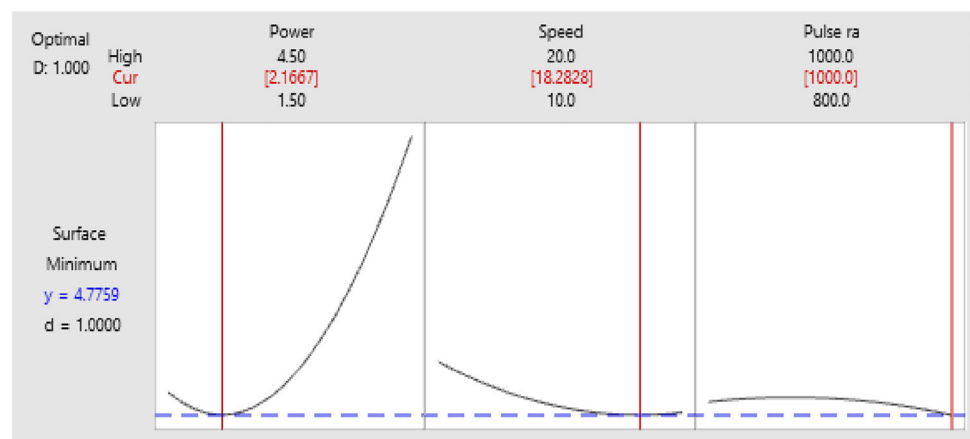
According to the normal probability plot for surface roughness (Fig. 7), the values of surface roughness are scat-

tered but close to the fitted line with no sign of skewness and non-normality. Therefore, the developed model is highly accurate in predicting the values of surface roughness. The straight line followed by the residuals is the reference for determining the errors in the model at any given point (Abidi et al. 2021).

3.5 Validation of the optimization results

To prove the practicality and, therefore, the feasibility of the model, three validation experiments were conducted using the optimum values of the inputs: 2.1667 W, 18.2828 mm/s, and 1000 PPI. The average value of surface roughness obtained was 4.6541 μm. The value was compared with the predicted value which is the optimum value (4.7759 μm).

Fig. 6 Optimization of surface roughness



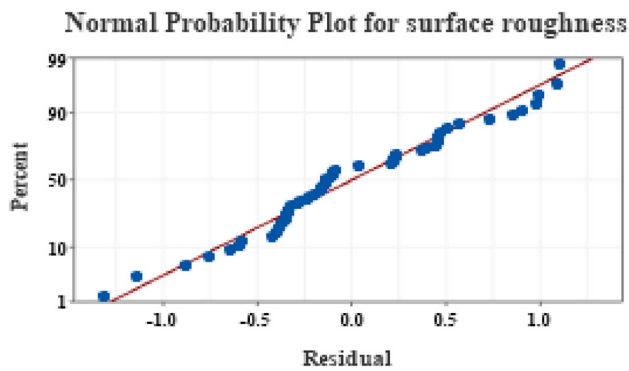


Fig. 7 Normal probability plot for surface roughness

The absolute percentage error (APE) was calculated using Eq. 2.

$$APE = \left| \frac{\text{Experimental value} - \text{predicted value}}{\text{Experimental value}} \right| \times 100\% \quad (2)$$

APE was found to be 2.617%. As shown in Fig. 8, the values of surface roughness predicted by the model are very close to the experimental values. This indicates the high accuracy of the model.

4 Conclusion

The study employed response surface methodology (RSM) to examine the effects of power, speed, and pulse rate on surface roughness in CO₂ laser ablation of PMMA substrates coated with 99.95% pure aluminium for microfluidic applications. ANOVA was performed. Optimization of the parameters was done, and the results were validated. A model for predicting

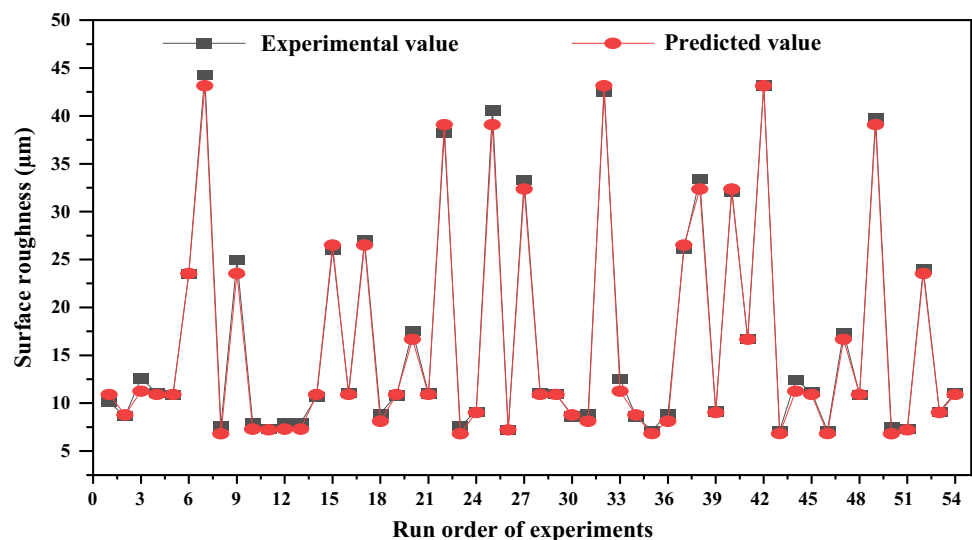
the values of surface roughness was developed and tested. Surface roughness is affected by the inputs and their interactions. Low values of power and high values of both pulse rate and speed give small values of surface roughness, and, therefore, high-quality microchannels.

The validation experiments show that the predicted values of surface roughness are very close to the experimental values. Hence, the developed model sufficiently predicts the values of surface roughness with a high degree of accuracy. The desired values of surface roughness can, therefore, be attained using the model. The results of the study show that RSM is an effective modelling and optimization technique for selecting the values of inputs and predicting the values of responses. The developed model can be benchmarked for validating other optimization models. The findings can further be used to develop technical guidelines for fabricating highly efficient and high-quality microchannels on PMMA.

For future work, comparative studies should be done with the Taguchi method and full factorial design. The study should be extended to also consider other shapes of microchannels, other substrate materials, and other inputs like the focal position of the lens, the number of laser passes, varying different thicknesses of the aluminium coating and workpiece, pulse width, pulse frequency, air pressure, and stand-off-distance. The other responses like kerf width, depth, dimensional deviation, aspect ratio, burr height, and burr width should also be studied. Analysis of surface roughness using a scanning electron microscope (SEM) should be done. Analytical modelling and finite element analysis should be employed to study the effects of the aluminium coating thickness on surface roughness.

Acknowledgements The authors gratefully appreciate the support of the Science and Technology Development Fund (STDF-12417) project. Special appreciation is extended to JICA for the TICAD7 scholarship offered to the first author. The authors are exceptionally grateful to

Fig. 8 Comparison of the experimental and predicted values of surface roughness



Asmaa Wadee, Shima Elsayed Ibrahim, and Moataz Abdel Karim for their incredible support.

Author Contribution JLO: conceptualization, methodology, software, data curation, visualization, formal analysis, investigation, validation, writing—original draft preparation. AMFE-B: supervision, resources, project administration, writing—reviewing, and editing. MY: supervision, writing—reviewing, and editing. HAE-H: supervision, resources, project administration, writing—revision, and editing.

Funding The authors declare that no funds, grants, or other support were received during the preparation of this manuscript.

Data availability All data generated or analysed during this study are included in this published article.

Declarations

Conflict of interest The authors declare that they have no known competing financial interests or personal relationships that could have appeared to influence the work reported in this paper.

References

- Abidi A, Ben Salem S, Yaltese MA (2021) Machining quality of high speed helical milling of carbon fiber reinforced plastics. *Proc Inst Mech Eng C J Mech Eng Sci*. <https://doi.org/10.1177/09544062211996736>
- Acherjee B, Kuar AS, Mitra S, Misra D, Acharyya S (2012) Experimental investigation on laser transmission welding of PMMA to ABS via response surface modeling. *Opt Laser Technol* 44(5):1372–1383. <https://doi.org/10.1016/j.optlastec.2011.12.029>
- Ali U, Karim KJBA, Buang NA (2015) A review of the properties and applications of poly (methyl methacrylate) (PMMA). *Polym Rev* 55(4):678–705. <https://doi.org/10.1080/15583724.2015.1031377>
- Aravind T, Boominathasellarajan S, Arunachalam N (2021) Fabrication of micro-channels on polymethyl methacrylate (PMMA) plates by thermal softening process using nichrome wire: tool design and surface property evaluation. *Proc Manuf* 53:182–188. <https://doi.org/10.1016/j.promfg.2021.06.088>
- Benton M, Hossan MR, Konari PR, Gamagedara S (2019) Effect of process parameters and material properties on laser micromachining of microchannels. *Micromachines (basel)*. <https://doi.org/10.3390/mi10020123>
- Choudhury IA, Shirley S (2010) Laser cutting of polymeric materials: an experimental investigation. *Opt Laser Technol* 42(3):503–508. <https://doi.org/10.1016/j.optlastec.2009.09.006>
- Dudala S, Rao LT, Dubey SK, Javed A, Goel S (2019) Experimental characterization to fabricate CO₂ laser ablated PMMA microchannel with homogeneous surface. *Mater Today Proc* 28:804–807. <https://doi.org/10.1016/j.matpr.2019.12.302>
- Eltawahni HA, Olabi AG, Benyounis KY (2010) Effect of process parameters and optimization of CO₂ laser cutting of ultra high-performance polyethylene. *Mater Des* 31(8):4029–4038. <https://doi.org/10.1016/j.matdes.2010.03.035>
- Hao HJ, Wang ML, Hao FQ (2013) Multi-objective optimization of quality in laser cutting based on response surface model. *Adv Mater Res* 756–759:3712–3716. <https://doi.org/10.4028/www.scientific.net/AMR.756-759.3712>
- Helmy MO, Fath El-Bab AM, El-Hofy H (2015) Elimination of clogging in PMMA microchannels using water assisted CO₂ laser micromachining. *Appl Mech Mater* 800:407–412. <https://doi.org/10.4028/www.scientific.net/amm.799-800.407>
- Helmy MO, El-Bab ARF, El-Hofy HA (2018) Fabrication and characterization of polymethyl methacrylate microchannel using dry and underwater CO₂ laser. *Proc Inst Mech Eng Part N J Nanomater Nanoeng Nanosyst* 232(1):23–30. <https://doi.org/10.1177/2397791417749700>
- Imran HJ, Hubeatir KA, Al-Khafaji MM (2021) CO₂ laser micro-enchancing of PMMA complemented by Taguchi and ANOVA methods. *J Phys Conf Ser*. <https://doi.org/10.1088/1742-6596/1795/1/012062>
- Khamar P, Prakash S (2020) Investigation of dimensional accuracy in CO₂ laser cutting of PMMA. *Mater Today Proc* 28:2381–2386. <https://doi.org/10.1016/j.matpr.2020.04.711>
- Konari PR, Clayton YD, Vaughan MB, Khandaker M, Hossan MR (2021) Experimental analysis of laser micromachining of microchannels in common microfluidic substrates. *Micromachines (basel)* 12(2):1–13. <https://doi.org/10.3390/mi12020138>
- Madić M, Mladenović S, Gostimirović M, Radovanović M, Janković P (2020) Laser cutting optimization model with constraints: maximization of material removal rate in CO₂ laser cutting of mild steel. *Proc Inst Mech Eng B J Eng Manuf* 234(10):1323–1332. <https://doi.org/10.1177/0954405420911529>
- Moradi M, Mehrabi O, Azdast T, Benyounis KY (2017) Enhancement of low power CO₂ laser cutting process for injection molded polycarbonate. *Opt Laser Technol* 96:208–218. <https://doi.org/10.1016/j.optlastec.2017.05.022>
- Nasser GA, Fath El-Bab AMR, Mohamed H, Abouelsoud A (2019) Low cost micro-droplet formation chip with a hand-operated suction syringe. *Proceedings—2018 IEEE 18th International Conference on Bioinformatics and Bioengineering, BIBE 2018*, pp 73–78, doi: <https://doi.org/10.1109/BIBE.2018.00021>.
- Okello JL, El-Bab AMRF, Yoshino M, El-Hofy HA, Hassan MA (2022) Modelling of surface roughness in CO₂ laser ablation of aluminium-coated polymethyl methacrylate (PMMA) using adaptive neuro-fuzzy inference system (ANFIS). *Adv Manuf*. <https://doi.org/10.1115/IMECE2022-92024>
- Oladoye AM, Carton JG, Benyounis K, Stokes J, Olabi AG (2016) Optimisation of pack chromised stainless steel for proton exchange membrane fuel cells bipolar plates using response surface methodology. *Surf Coat Technol* 304:384–392. <https://doi.org/10.1016/j.surfcoat.2016.07.023>
- Prakash S, Kumar S (2015) Fabrication of microchannels on transparent PMMA using CO₂ Laser (10.6 μm) for microfluidic applications: an experimental investigation. *Int J Precis Eng Manuf* 16(2):361–366. <https://doi.org/10.1007/s12541-015-0047-8>
- Prakash S, Kumar S (2015) Fabrication of microchannels: a review. *Proc Inst Mech Eng B J Eng Manuf* 229(8):1273–1288. <https://doi.org/10.1177/0954405414535581>
- Prakash S, Kumar S (2017) Experimental and theoretical analysis of defocused CO₂ laser microchanneling on PMMA for enhanced surface finish. *J Micromech Microeng*. <https://doi.org/10.1088/1361-6439/27/2/025003>
- Prakash S, Kumar S (2018) Pulse smearing and profile generation in CO₂ laser micromachining on PMMA via raster scanning. *J Manuf Process* 31:116–123. <https://doi.org/10.1016/j.jmapro.2017.11.003>

- Prakash S, Acherjee B, Kuar AS, Mitra S (2013) An experimental investigation on Nd:YAG laser microchanneling on polymethyl methacrylate submerged in water. *Proc Inst Mech Eng B J Eng Manuf* 227(4):508–519. <https://doi.org/10.1177/0954405412472178>
- Umbrecht F et al (2009) Solvent assisted bonding of polymethylmethacrylate: characterization using the response surface methodology. *Sens Actuators A Phys* 156(1):121–128. <https://doi.org/10.1016/j.sna.2009.03.028>

Publisher's Note Springer Nature remains neutral with regard to jurisdictional claims in published maps and institutional affiliations.

Springer Nature or its licensor (e.g. a society or other partner) holds exclusive rights to this article under a publishing agreement with the author(s) or other rightsholder(s); author self-archiving of the accepted manuscript version of this article is solely governed by the terms of such publishing agreement and applicable law.